Investigating a loss of Magnetic Domain Memory in a [Co/Pd]/IrMn Thin film

Mason L. Parkes

A senior thesis submitted to the faculty of
Brigham Young University
in partial fulfillment of the requirements for the degree of

Bachelor of Science

Dr. Karine Chesnel, Advisor

Department of Physics and Astronomy

Brigham Young University

ABSTRACT

Investigating a loss of Magnetic Domain Memory in a [Co/Pd]/IrMn Thin film

Mason L. Parkes
Department of Physics and Astronomy, BYU
Bachelor of Science

An investigation is made into the effect that certain parameters, such as smoothing tolerance and integration ellipse size, used to determine the degree of magnetic domain memory (MDM), have on the level of MDM observed. Decreasing the tolerance which results in more smoothing, and increasing the size of the integration ellipse both cause higher levels of MDM. Careful pairing of ellipse size and tolerance yields MDM maps with far higher degrees of observed MDM than maps that were originally generated for the series analyzed.

This pairing of parameters yields MDM in the zero field cooling (ZFC) series examined to be higher than in the 5000 G field cooled (5000 G FC) series. This is consistent with previous results (Chesnel et al. 2016) and indicates that increased MDM in these maps is not purely artificial.

While certain parameters were found to increase the degree of MDM, they still did not reach levels previously observed in this sample, and the search for a physical cause for the loss of MDM continues through efforts to investigate the effect of x-ray illumination on MDM.

Keywords: Magnetic Domain Memory

ACKNOWLEDGMENTS

I'd like to thank my advisor, Dr. Chesnel. I took her modern physics class when I was considering changing paths away from a career in physics, but my experience in that class and learning from her example in her research group has inspired me to pursue graduate studies in physics. I'd also like to thank all the other wonderful professors in the BYU Department of Physics and Astronomy for the time they took to help me understand the concepts I've learned.

I am also increadibly grateful to my parents and grandparents for the examples they have been and how they've helped me see the importance of learning. I could not have done this without their support.

Finally, I would like to thank my wife. She has always believed in me, and when I've been intimidated by an assignment or there was some task I didn't think I was equal to, her support was always there to help me accomplish things I never could have otherwise.

Contents

Chapter 1

Introduction

This introduction includes an overview of the material studied, key physical concepts, including Magnetic Domain Memory, that are investigated and the experimental procedures used to do so. Also provided is a look at more recent data that exhibits a loss of Magnetic Domain Memory under conditions where it was expected.

1.1 Material

The material consists of a multilayered film based on the stacking of a Co/Pd multilayer with an IrMn alloy layer. The Co/Pd consists of 12 layers of cobalt, each 7 Å thick, separated by layers of palladium, each 12 Å thick. There are 4 such Co/Pd multilayers, and each is separated by a 24 Å layer of Iridium Manganese alloy. (see Fig 1.1). The sample was fabricated in the group of Prof. Eric Fullerton at the University of California, San Diego, CA. It has potential applications in data storage.

This material exhibits interesting properties that will be discussed further in later sections due to coupling at the interfaces between ferromagnetic and antiferromagnetic parts of the sample.

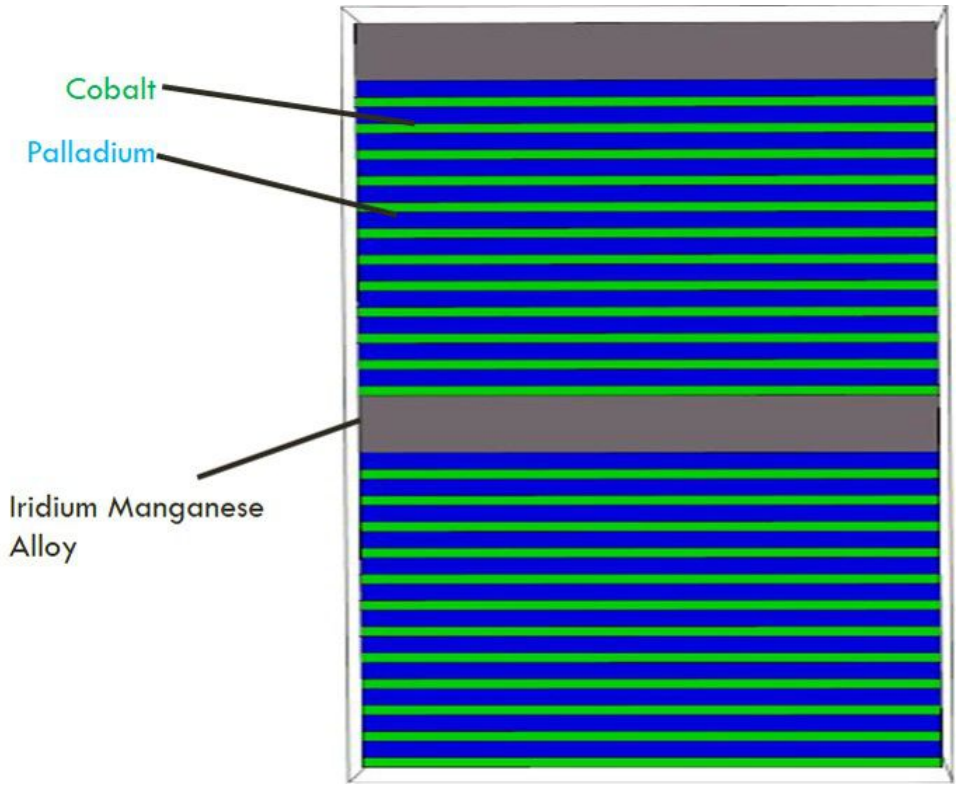

Figure 1.1 A labeled diagram of the sample, showing the ferromagnetic 7 Å cobalt layers between 12 Å palladium layers, repeated 12 times, followed by a 24 Å layer of antiferromagnetic iridium manganese alloy. This structure is then repeated four times. This illustration shows half of the sample.

1.2 Magnetic Domains and Hysteresis

When the sample is placed in an external magnetic field, the atomic spins carried by the Co atoms within the ferromagnetic portion of the sample will align with the external field. Groups of spins that all point in the same direction within the sample are referred to as a magnetic domains. Due to the way the layers are situated within the sample, magnetic domains align perpendicular to the surface of the material, that is, the films exhibit perpendicular magnetic anisotropy (PMA). When the net magnetization is near zero, the domains within the sample are oriented in such a way that equal parts point up and down.

As an external field is applied, spins within the sample will align with it and the sample will acquire a non-zero net magnetization. This net magnetization will increase as domains pointing in the direction of the applied field grow in size until they cover the entire film. At that stage the sample's magnetization has reached a maximum value (saturation point, point 1 on Fig. 1.2). When the applied magnetic field decreases in strength from saturation, magnetic interactions within the sample will keep domains aligned longer. When the field reaches a lower value, called the nucleation point (point 2 in Fig. 1.2), new domains with magnetization pointing in opposite to the applied field start to nucleate.

As the applied field continues to decrease in strength down to zero (descending branch of the magnetization loop), the sample may still exhibit some non-zero net magnetization because the arrangement of domains within the sample is history dependent. If a magnetic field is then applied in the opposite direction, the film will eventually exhibit zero net magnetization (point 3 in Fig. 1.2). This point is called the coercive point. If the magnitude of this applied field continues to increase in the opposite direction, the domains within the sample will continue to expand until they cover the entire film. The sample has now reached saturation in the other direction (point 4 in Fig. 1.2). Returning to zero applied field (ascending branch) yields a symmetrical behavior. It remains at saturation until nucleation occurs (point 5 in Fig. 1.2) and spins begin to switch to the

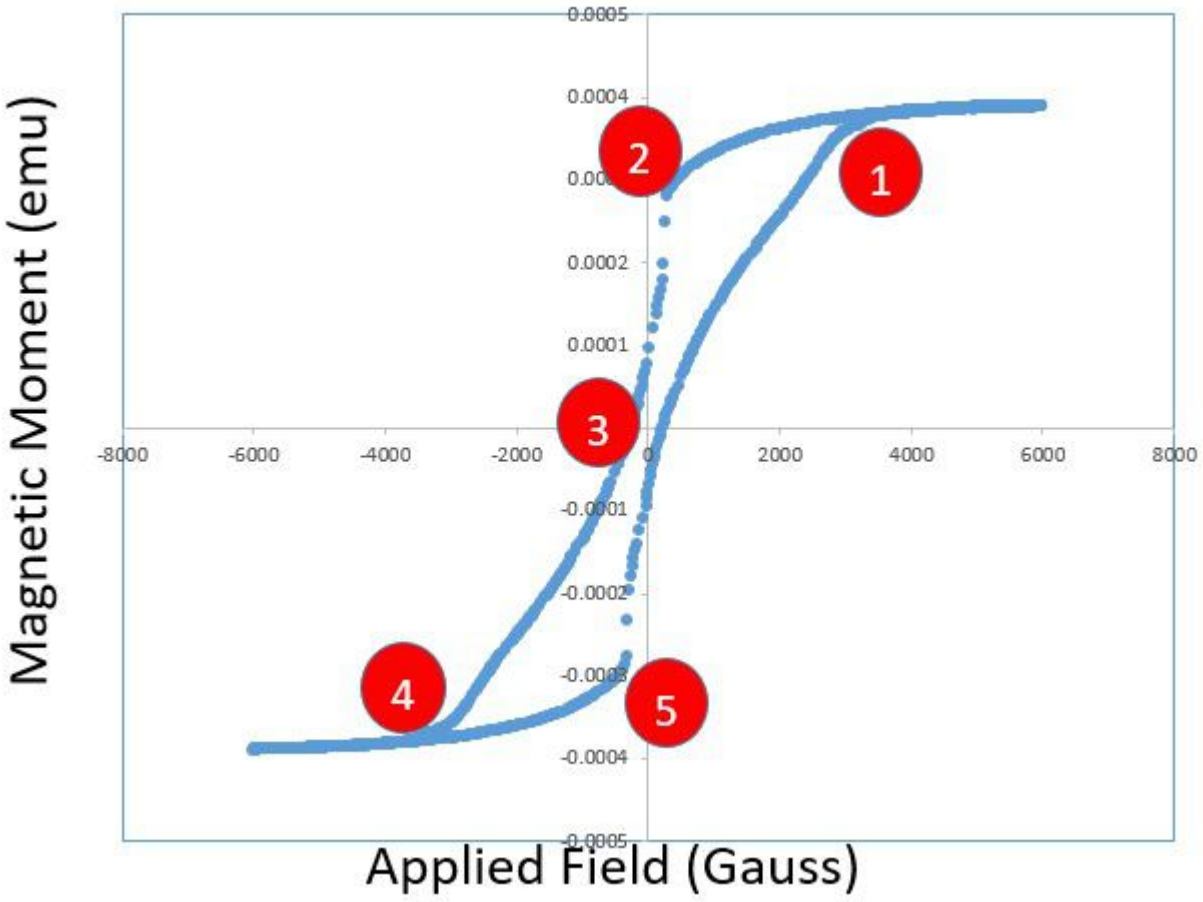

Figure 1.2 This plot shows how the magnetization of the sample responds to an applied magnetic field. Points are labeled where noteworthy phenomena occur. 1-Saturation is reached as all domains within the sample point in one direction. 2-Nucleation begins as spins within the sample begin to form domains pointing in the other direction. 3-Coercive Point, the sample has no net magnetization and domains within it are balanced. 4- Saturation is reached in the other direction as all spins now point opposite the direction they did at point 1. 5-Nucleation begins in the other direction, and new domains begin to form in that direction.

initial direction and form new domains.

In general, these domains can form anywhere in the sample. There is no set location for domains to nucleate. The process of spins flipping between aligned with the applied field and pointed the opposite direction is driven by a balance between magnetic interactions, the structure and shape of

the material, as well as thermal energy, which leads to a somewhat probabilistic process. Given the large numbers of atomic spins in the film, it is unlikely that the same pattern of magnetic domains will repeatedly occur while cycling the applied magnetic field.

1.3 Magnetic Domain Memory

Magnetic Domain Memory (MDM) is the term used to describe when the magnetic domain pattern within the film returns to the same configuration at the same field value after the field has been cycled, even all the way to saturation. In general, the domain pattern at one applied field value does not match with the domain pattern at the same field value after cycling the field, only the average size of the domains is the same, but not their spatial configuration (topology). When MDM is exhibited, the size and orientation of the domains is the same, but so is the specific domain pattern.

The degree to which MDM occurs can vary. Partial MDM can be observed when the initial and final domain patterns are similar, or complete MDM can occur if the domain patterns are exactly the same. The physical phenomenon causing MDM often dictates whether it is complete or partial.

This remarkable property can only occur in certain situations. In our [[Co/Pd]/IrMn] sample, MDM occurs because of couplings between the ferromagnetic [Co/Pd] layers and the antiferromagnetic IrMn layers. In order to observe MDM in this type of system, it must be cooled below a blocking temperature. The field that is applied while the sample is cooled has a large effect on the level of MDM observed. It has been previously shown (Chesnel 2017), that under zero-field-cooling (ZFC) conditions (i.e., when the sample is cooled down in the absence of an external field), almost 100% MDM is reached throughout much of the magnetization loop. The couplings between layers that lead to MDM are also responsible for an exchange bias, a lateral shift in the hysteresis loop of the sample when collected after being cooled below the blocking temperature under a large applied field.

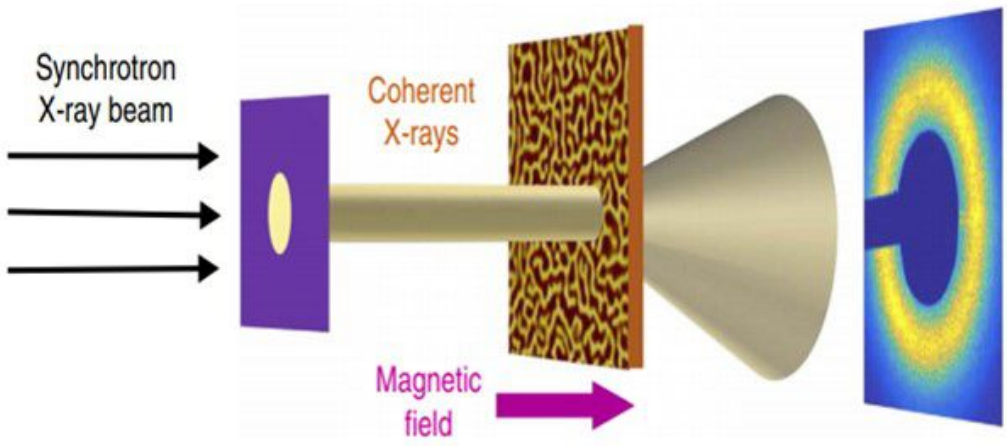

Figure 1.3 A diagram of coherent x-ray resonant magnetic scattering experiment, showing x-rays from the synchrotron passing though a pinhole to induce coherence before striking the sample. The sample is exposed to a magnetic field, and the resulting scattering pattern is collected on a CCD detector.(Chesnel et al. 2016)

1.4 Magnetic Speckle Correlation Technique

It is possible to measure MDM by observing the domains directly in real space. Magnetic force microscopy (MFM) allows to image the magnetic domain patterns via detecting the magnetic stray field perpendicular to the surface of the film. With MFM, it is possible to apply fields and take images of the domain patterns in the same part of the sample at various field values. However, our MFM instrument does not offer cooling capability necessary for measurements below the blocking temperature for our system.

We rely on another method of measuring MDM, using coherent x-rays and the technique of magnetic scattering. When coherent x-rays strike the sample, the magnetic domain pattern produces as speckled scattering pattern, which can be collected on a CCD camera. Due to the coherent nature of the light, this speckle pattern is unique to the specific magnetic domain pattern. Such an experiment is illustrated in Fig. 1.3.

The x-rays are not affected by the applied magnetic field, so these speckle patterns can be

collected while a magnetic field is applied. Additionally, cooling the film is possible by mounting it onto a cryostat. A further advantage is that by tuning the x-ray energy to resonant edges, specific elements (such as Co) within the sample can be probed. Finally, thanks to an internal in-situ magnetic field, speckle patterns can be collected for many different field values, providing the opportunity to compare the magnetic domain patterns at different field values.

Once collected, the speckle patterns provide a unique fingerprint of the domain pattern within the film. To evaluate the level of similarity between two domain patterns through their respective speckle patterns, a process called cross-correlation is used. Cross-correlation compares two speckle patterns, collected at different field values, and creates a cross-correlation pattern. Once integrated the cross-correlation signal provides with a correlation coefficient between 0 and 1 that relates to the amount of MDM present–a coefficient of 1 corresponding to 100% MDM and a coefficient of 0 corresponding to no MDM, the domains in the sample are completely different.

As the cross-correlation process is completed for the many images collected throughout the magnetization cycle, a collection of correlation coefficients is generated. These correlation coefficients can be mapped out in the magnetic field space. On such a map(see Fig. 1.4) the axes are the field values where the different images were collected, and the color scale represents the correlation coefficient, or the degree of MDM.

1.5 Observed Loss of MDM

Data collected at the Advanced Light Source (ALS) in Berkeley, California has shown that the sample can exhibit up 100% MDM throughout most of the magnetization loop. (Chesnel et al. 2016) However more recent data collected at the Advanced Photon Source (APS) at Argonne National Laboratory has shown lower levels of MDM. In my research, I have focused on two specific series of data that were collected in November of 2016 at the APS. These two series are labeled as the

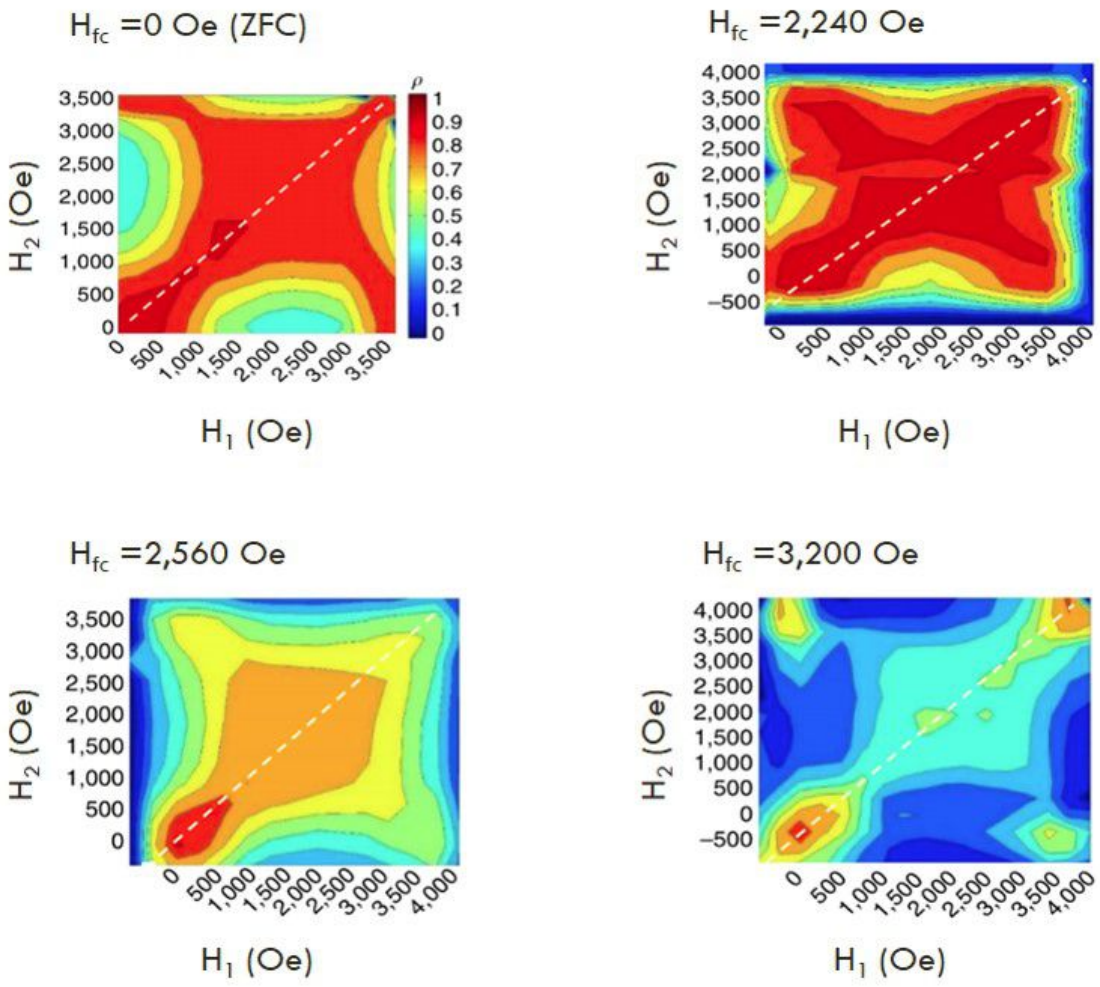

Figure 1.4 A selection of MDM maps from from Dr. Chesnel's 2016 Nature Communications article showing the high degree of MDM made possible through a wide range of magnetic field values as a result of proper field cooling conditions. Each axis corresponds to the field value when one image was taken, the color corresponds to the level of correlation between the two images. The images compared in these maps are all seperated by a full cycling of the magnetic field, so that domains have been completely destroyed by a saturating field in the opposite direction.(Chesnel et al. 2016)

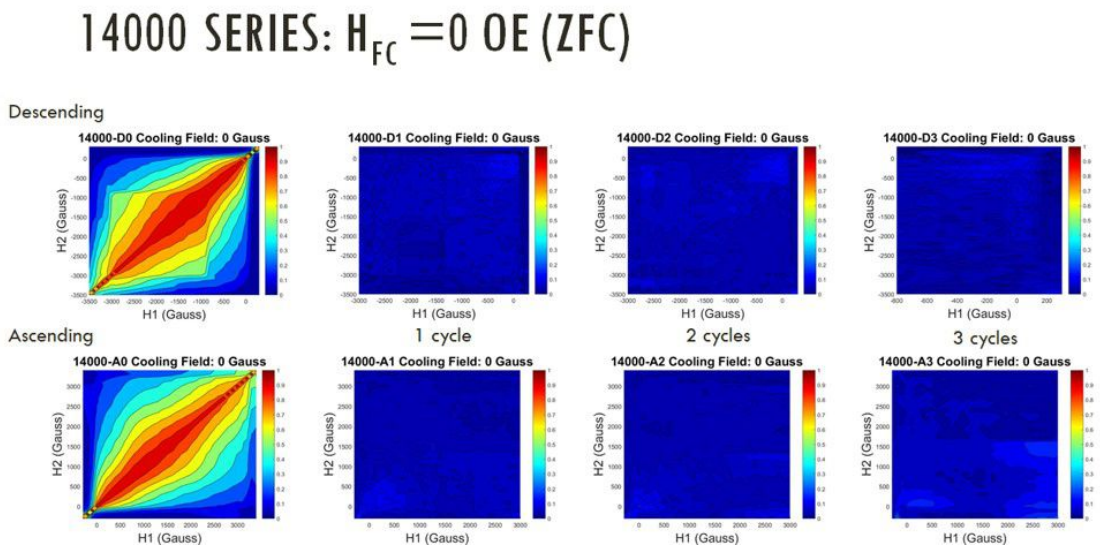

Figure 1.5 MDM maps generated from data taken at the APS that showing much less MDM than observed in previous experiments. Here, the maps to the left show the correlation between images on the same cycle, each image to the right shows the correlation between images collected seperated by an additional saturating field in the other direction. The top row shows correlations between images taken for descending field values and the bottom row for ascending field values. The completely blue appearance of all maps past the first indicate a complete loss of magnetic domain memory.

14000 series, which was collected in ZFC conditions, and the15000 series, which was collected after cooling under a 5000 G field. Previous results have shown that the most MDM is achieved under ZFC conditions, and so it is expected that data from the 14000 series should show a high level of MDM, while data from the 15000 series should show MDM occurring to a lesser degree.

Chapter 2

Investigating the Effect of Parameters used in Speckle Correlation Technique

There were no readily identifiable physical differences that could explain the complete disappearance of MDM in the type of sample where it had previously been observed to be nearly complete throughout large areas of the magnetization loop. Additionally, the CXRMS experiments where this data was collected are difficult to complete because the receiving time at synchrotron beamlines is competitive and the set up for such experiments that allow the cooling of the material to very low temperatures and the application of high magnetic fields is very complex. As a result, I thoroughly investigated the effects that certain parameters used in the processing and analysis of data had on the MDM maps that were produced.

The following section contains more detail about the MatLab program used to analyze the images collected from scattering experiments, and describe my efforts to determine if better tuning parameters within this program could result in the observation of higher degrees of MDM in the sample.

2.1 A closer look at data processing methods

There are several key steps that must be performed to generate an MDM map from a series of CXRMS images collected while cycling through a magnetic field. The first that deserves full attention is the separation of the coherent and incoherent part of the signal.

2.1.1 Smoothing

It was previously mentioned that coherent light is essential because it produces a speckle pattern that is a unique fingerprint of the magnetic domain configuration in real space. However, the actual coherence of the beam is far from ideal. As a result, much of the signal that we measure is from scattered incoherent light. This scattered light provides information of the long range magnetic ordering, which is an average over the sample.

The incoherent portion of the light produces speckle spots uniformly distributed throughout the scattering pattern. To remove this part of the signal, the raw data is smoothed–averaged with the points around it–until a specified tolerance is met. For each step, the data is smoothed and the resulting smoothed data is subtracted from the raw data. The difference is the pure speckle pattern that contains the pattern unique to the domain configuration in real space. The tolerance is met when the second derivative of the speckle amplitude with respect to the number of smoothing passes drops below the aforementioned tolerance. A lower tolerance means that more smoothing will occur and more of the data will be averaged as the coherent part of the signal.

After smoothing, only the coherent part of the signal that contains unique information about the domain configuration of the sample is left. (see Fig. 2.1)

Often, several tolerances are compared so that the ideal level of smoothing can be determined. Once this tolerance is chosen, all images in a given series undergo the same process using the same optimized tolerance, and the resulting pure speckle patterns are ready to be compared. This allows

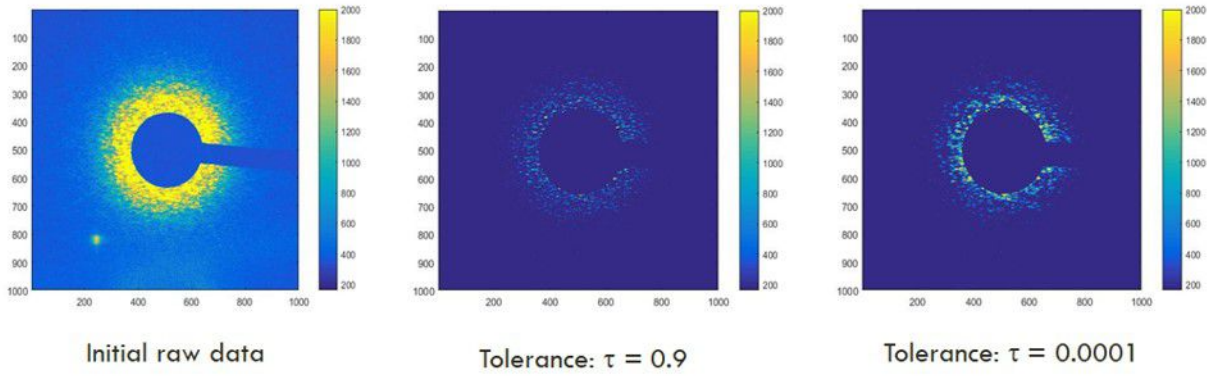

Figure 2.1 The leftmost image shows raw data collected as a CXRMS image. The center and rightmost image show the coherent signal extracted after smoothing for two seperate tolerances. There is a clear difference in the speckle size obtained depending on the tolerance.

the comparison of unique domain configurations, not just a comparison of net magnetizations, which will, of course, be the same for a given applied field each time that value is reached in the cycle.

2.1.2 Cross-correlation

After the smoothing procedure is completed, the speckle patterns are cross-correlated. Each speckle pattern is compared with every other speckle pattern. This comparison yields the cross-correlation peaks shown in Fig. 2.4. It is worth noting that the axes of these cross-correlation patterns are pixels. The height of the pattern at each pixel coordinate represents how similar the two speckle patterns are when one is shifted in respect to the other one by that amount of pixels. For example, the height of the center peak indicates how similar the two speckle patterns are when they are not shifted at all with respect to each other. A point one pixel over corresponds to a one pixel shift of one image with respect to the other in that direction. In this way, the width of the central peak is related to the average size of the speckle spots.

2.1.3 Integration

To determine amount of MDM, a correlation coefficient, whose value is between 0 and 1 is estimated by taking the area under the cross-correlation pattern and normalizing it to autocorrelation patterns. An integration ellipse is specified by the user and all relevant data are summed and divided by the square root of the product of correlating each speckle pattern with itself. This integration is then repeated for each cross-correlation pattern.

The resulting correlation coefficient measures how similar two speckle patterns, and therefore the arrangement of magnetic domains in the sample at two distinct field values, are. In order to visualize this data, MDM maps are created that compare images taken over one branch of a magnetization loop to images taken over another branch after the domains have been completely destroyed, either once or multiple times, by saturating the material in the other direction. In this way it is clearly visualized whether or not the domains in the sample have returned to the same exact configuration, indicated by a correlation coefficient close to 1 and the color red on the MDM map, or if they have an entirely different configuration, indicated by a correlation coefficient close to 0 and the color blue on the MDM map.

2.2 Effects of Varied Tolerance

As previously mentioned, during the smoothing process a tolerance is chosen that the program uses to determine when to stop smoothing the speckle pattern and separate the coherent and incoherent parts of the signal. This tolerance is generally chosen so that the coherent part of the signal which is to be subtracted is visually determined to match the overall envelope of the scattering signal, so the sharp speckle spots can be extracted.

In an effort to determine why the recent data of the 14000 and 15000 series did not exhibit the same levels of MDM as previous data, I varied this tolerance parameter and completed the

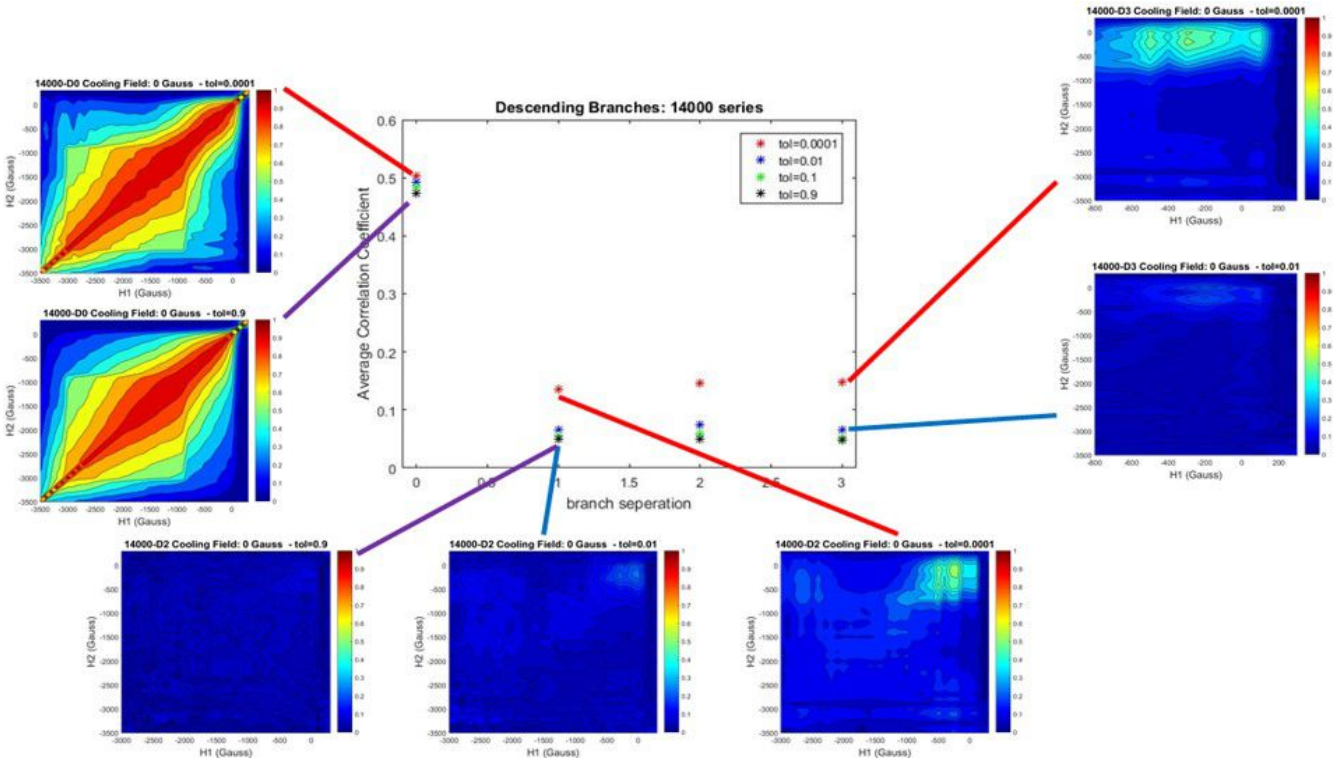

Figure 2.2 The center plot shows the average correlation coefficient on maps generated for a given tolerance at different branch seperations, or the number of opposite saturating fields between the images being compared. Around the center graph, colored lines link MDM maps to the corresponding point on the plot, allowing for a visual comparison of the effect tolerance has on MDM maps.

cross-correlation process for each series with different tolerance values.

By visual examination of the generated maps and by comparing the average values of the maps made with different tolerances one can observe a trend in the degree of MDM in respect to the tolerance value. (see Fig. 2.2 and Fig. 2.3) Over the range of tolerances explored here, roughly covering from 1 to $1x10^{-6}$, a great variation occurs in the degree of MDM. Maps created for branches with no separating cycles, where each image was compared with others within the same branch, were hardly affected by the different tolerances. When comparing with other branches higher levels of MDM appeared with a lower tolerance. These high MDM regions primarily coincided with the region of the map corresponding to nucleation.

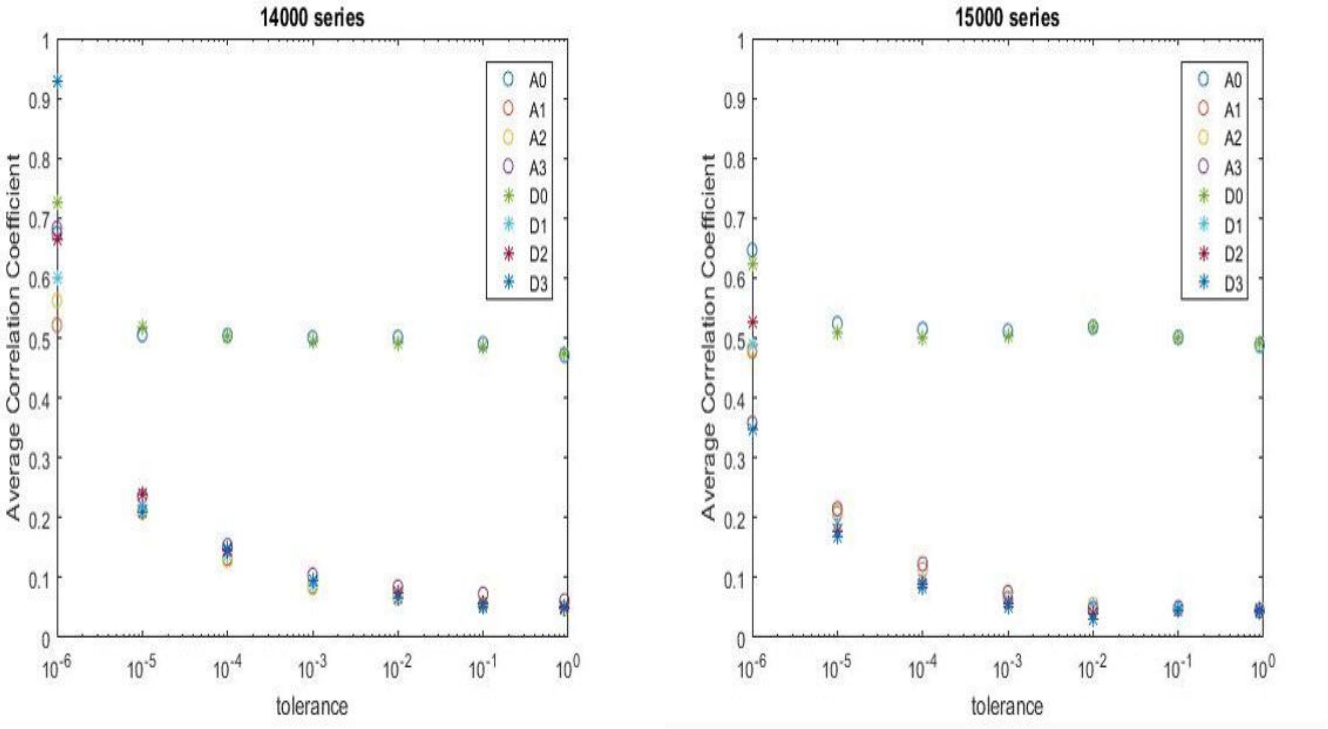

Figure 2.3 Each plot shows the average correlation coefficient found from MDM maps for a specific tolerance, each point is labelled A for ascending of D for descending and a number indicating the number of saturating field between images being compared. The plot on the left compares images in the 14000 (ZFC) series, while the plot on the left compares images in the 15000 (5000 G FC) series, each plot shows an increase in average MDM value with smaller tolerances, though the effect is more pronounced in the maps that initially showed very little MDM.

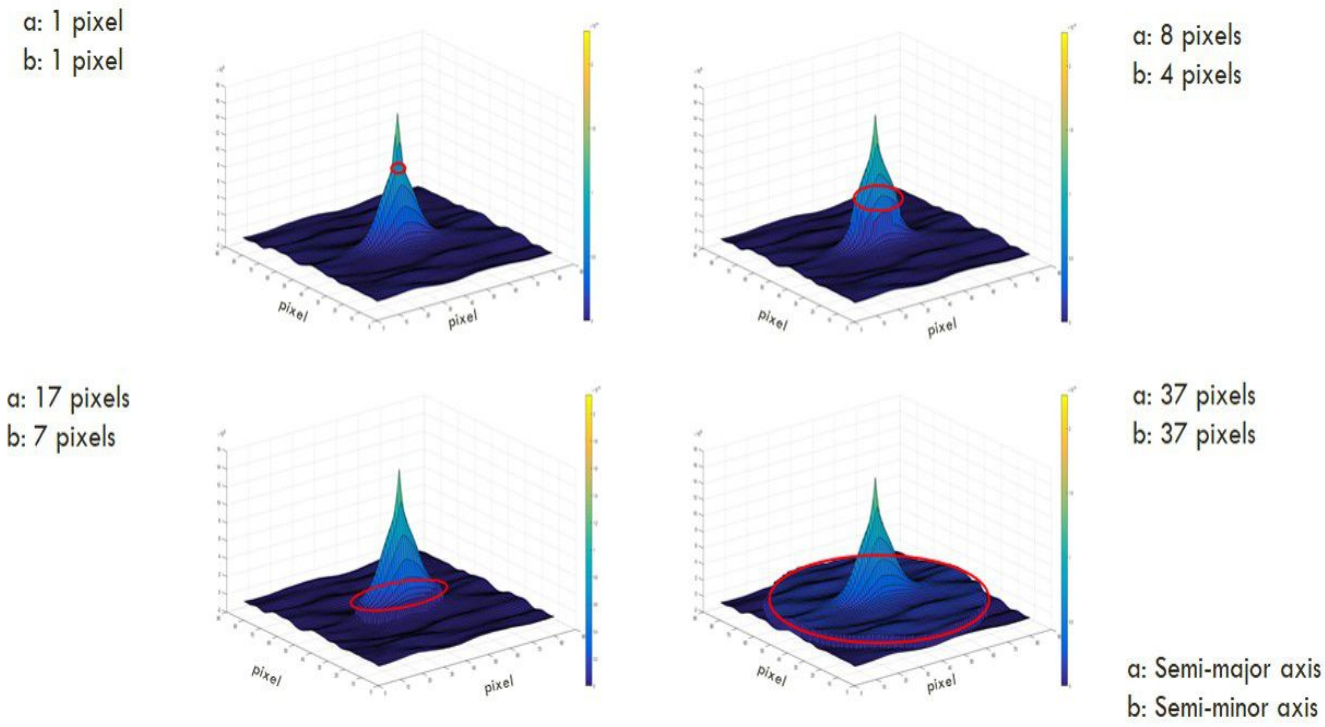

Figure 2.4 Each of the four images shows an example of the pattern generated by cross-correlating two images. The red ring on each image shows a selection of the different ellipse sizes used to investigate the effect ellipse size had on the MDM maps generated.

2.3 Effects of Varied Integration Ellipse Size

As with the selection of the smoothing parameter, the size of the integration ellipse is generally chosen arbitrarily. Because the width of the peak in the cross-correlation pattern is related to the average speckle size, which is determined by the optics of the experimental apparatus, the area to be integrated was usually selected as around the base of the peak, or something nearer the full width at half maximum. Selecting a larger integration area allows the inclusion of off-peak secondary undulations. (see Fig. 2.4)

As with the tolerance parameter, we found that varying the ellipse size had a large effect on the degree of MDM observed. The larger the integration ellipse specified, the greater the level of measured MDM. It should be especially noted that in this case the larger ellipses affect the degree of

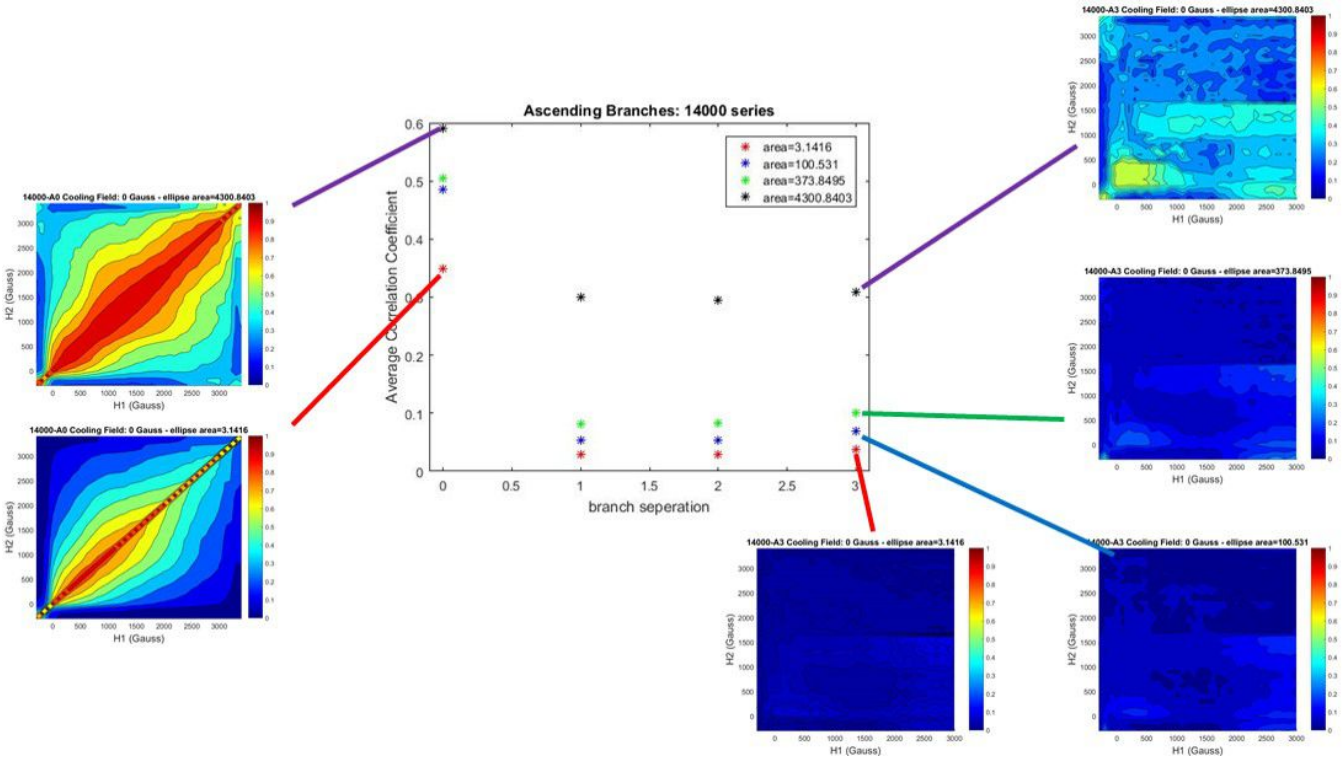

Figure 2.5 Similar to figure 2.2, points show the average correlation coefficient on maps generated at different loop separations and different ellipse sizes. Maps around the center plot allow a visual comparison of what a larger integration ellipse does.

MDM through broad areas of the map. It also has a noticeable effect on all branch separations, even the 0 separation branch where each image is correlated with another without the domains having been completely destroyed by a saturating field. (see Fig. 2.5 and Fig. 2.6)

2.4 Combined Effects of Varied Tolerance and Ellipse Size

Following the investigation of each parameter individually, I began an investigation to determine if some combination of tolerance and ellipse size could yield MDM maps similar to those generated from previous experiments. In this case, it is possible that the MDM is still present in some region of the hysteresis cycle, but our initial analysis was unable to find it.

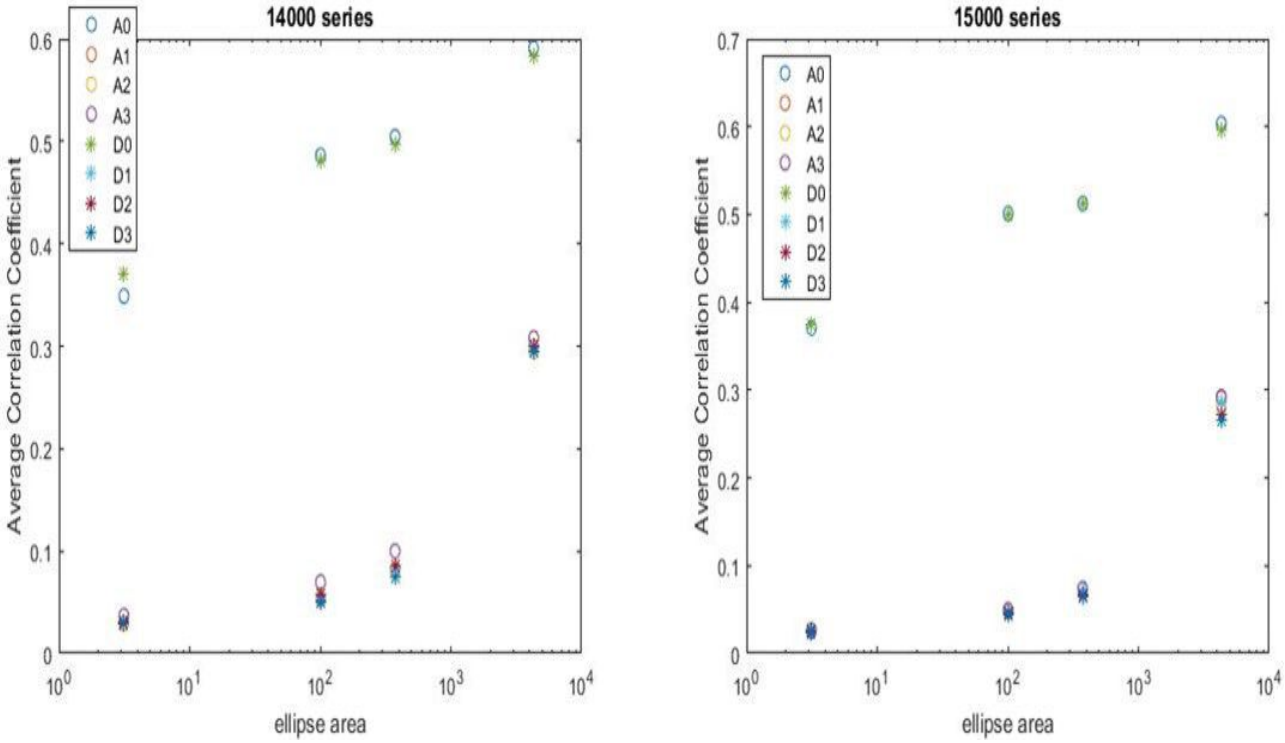

Figure 2.6 Similar to figure 2.3, but here the average correlation coefficient for several maps is plotted as a function of ellipse size. Again, the image on the left is for the ZFC series while that on the right is for the 5000 G FC series. A clear increase of apparent MDM follows an increased ellipse size for all images. Including the zero seperation images, which in the tolerance investigation showed little change for varied tolerance.

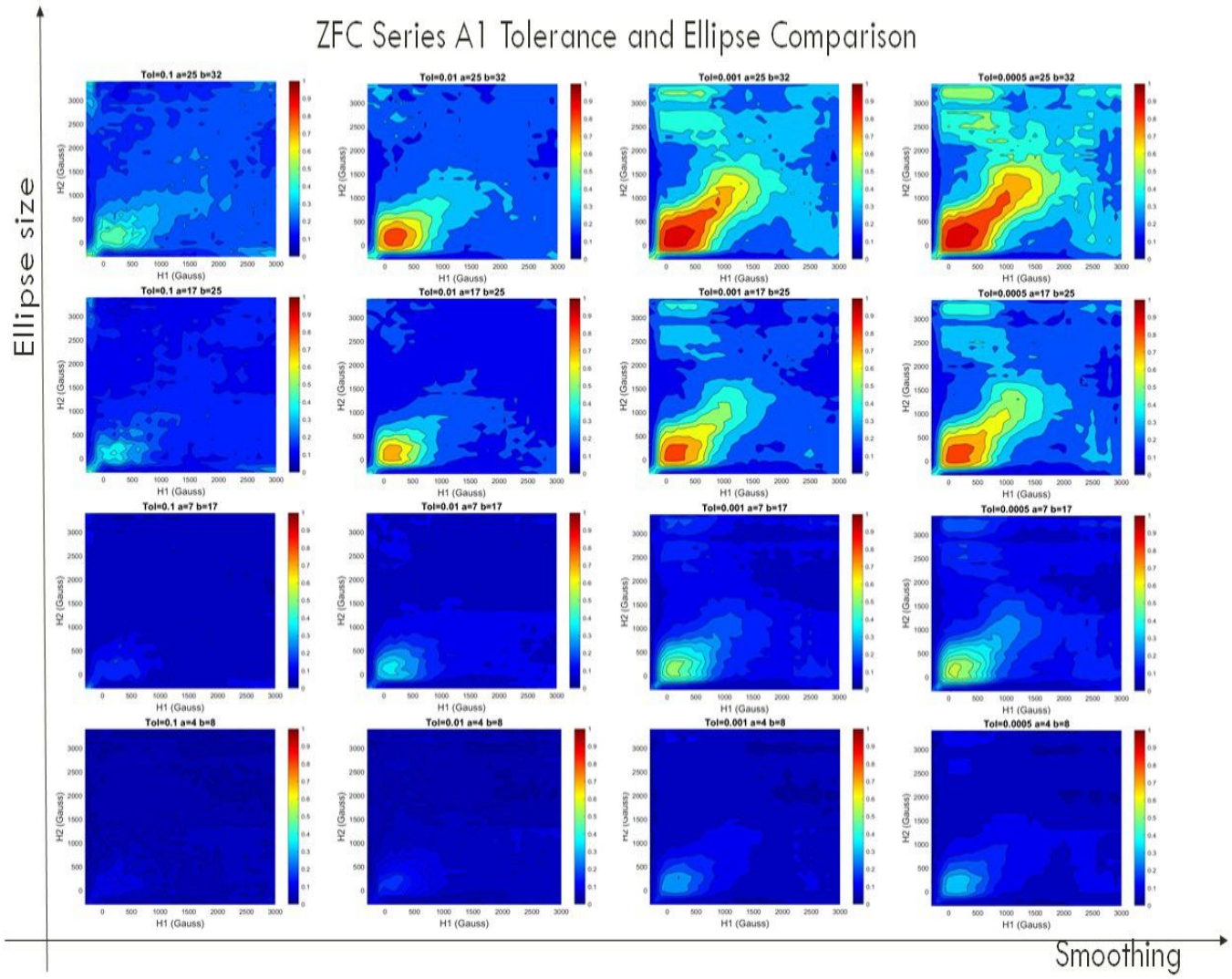

Figure 2.7 All 16 of these MDM maps were created from the same raw data in the 14000 (ZFC) series. Maps in the same column were generated using the same tolerance, those tolerances are, from left to right: 0.1, 0.01, 0.001, 0.0005. Maps in the same row were generated using the same integration ellipse. Those are (semi-minor axis, semi-major axis), from bottom to top: (4,8), (7,17), (17,25), (25,32). More MDM is apparent for larger ellipse sizes and for more smoothing, but in all cases it occurs most strongly when the two images being compared are near nucleation.

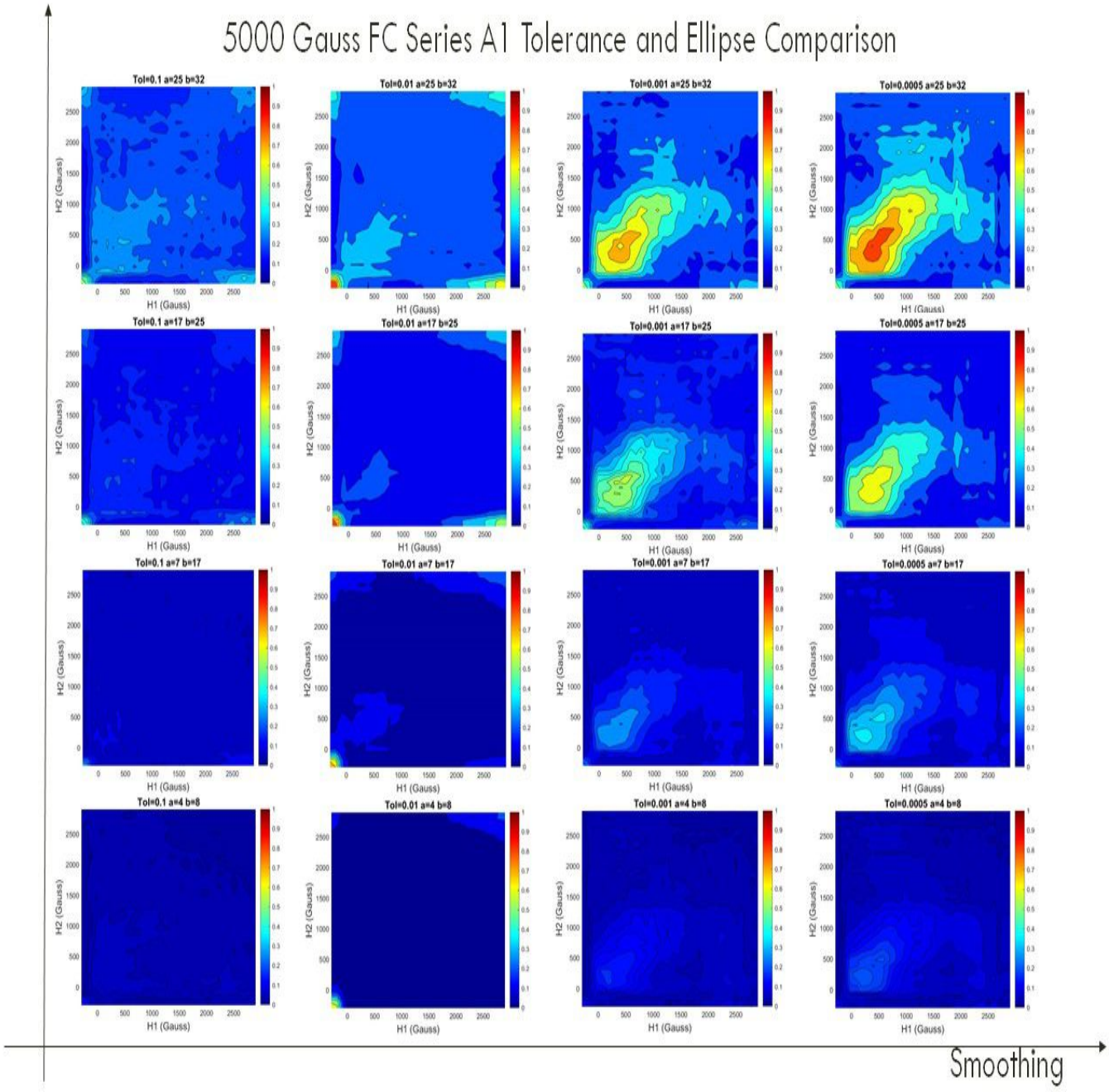

Figure 2.8 Similar to Fig. 2.7, but examining the effects of ellipse size and tolerance on data from the 15000 (5000 G FC) series. The same pattern for increased MDM is apparent; for larger ellipse sizes and for more smoothing, but in all cases it occurs most strongly when the two images being compared are near nucleation. Maps in the same column were generated using the same tolerance, those tolerances are, from left to right: 0.1, 0.01, 0.001, 0.0005. Maps in the same row were generated using the same integration ellipse. Those are (semi-minor axis, semi-major axis), from bottom to top: (4,8), (7,17), (17,25), (25,32).

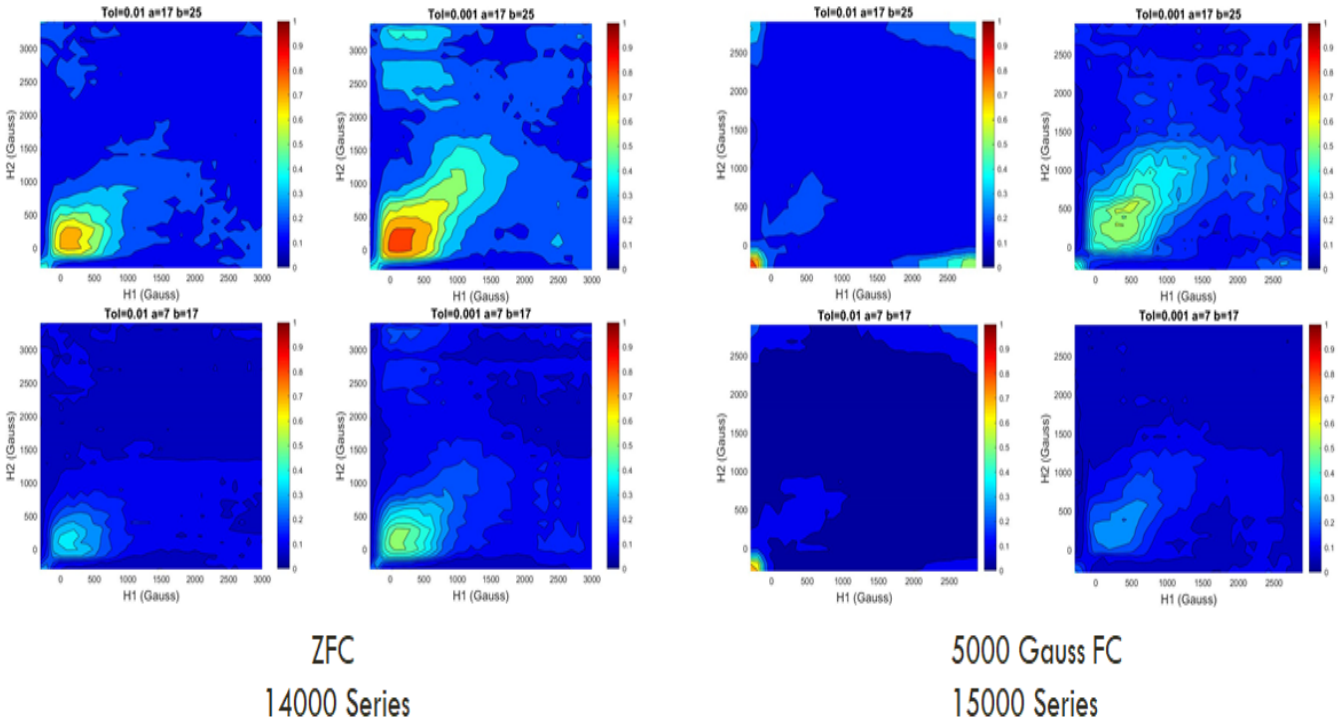

Figure 2.9 The 4 MDM maps from the centers of Fig. 2.7 (left) and 2.8 (right), showing a comparison of the same ellipse sizes and tolerance choices between the 14000 (ZFC) series (left) and 15000 (5000 G FC) series (right). Though observed MDM increases for both series depending on the selection of parameters, the effect is more noticable for the ZFC series, where more MDM was expected based on previous results. Ellipse sizes (semi-minor axis,semi-major axis) for the bottom rows are (7,17) and for the top rows are (17,25) while tolerance for the left columns is 0.01, with 0.001 for the right columns

From the comparison of multiple MDM maps made for each series, it is clear that for the same tolerance and ellipse size parameters (see Fig. 2.9), the 14000 series (prepared with ZFC) exhibits more MDM than the15000 series (prepared with a 5000 G cooling field). This result is consistent with previous measurements.

Furthermore, inspection of the resulting maps shows that for both series, what MDM does occur appears to start in the corner of the map that corresponds to near nucleation. (see Fig. 2.7 and Fig. 2.8) This indicates that the magnetic domains within the sample are most similar when they are first beginning to nucleate from being saturated in the other direction. This result is possibly explained by imperfections in the sample that would cause certain regions to behave as an anchor for magnetic domains to nucleate. Even without knowing what is causing that behavior, the fact that it is observed specifically in that region more than anywhere else leads to the conclusion that the increased degree of MDM after after carefully selecting the processing parameters is showing a physical source for the observed MDM, where such a pattern in another region of the map or on the entire map indiscriminately could indicate that increased levels of MDM are artificial.

Chapter 3

Conclusions

Careful selection of parameters used to generate MDM maps from data collected from two different field cooling conditions, ZFC and 5000 G FC, reveals that the selection of these parameters has a great effect on the level of MDM observed. Selecting lower tolerances and larger ellipse sizes both yield higher degrees of MDM in the associated maps, but lower tolerances seem to have a pronounced effect in map regions where higher MDM is expected, in other words, when both correlated images are near nucleation, while larger ellipse sizes cause a more widespread growth in MDM.

Throughout this investigation, I was still unable to find some pairing of parameters that would yield the levels of MDM observed in earlier series collected under the same magnetic field conditions but at different beamlines. Additionally, the investigation made no attempt to explain why special treatment would be needed for these series to exhibit the same levels of MDM seen in earlier data with larger tolerances and smaller ellipse sizes.

A possible resolution to this conflict is currently being investigated in our group as we make magnetotransport measurements of the sample throughout the CXRMS experiment described here in an effort to verify that the x-ray illumination of the sample has a possible effect on its magnetic behavior. It is possible that different intensities of light produced at the different beamlines could

in some cases destroy the exchange bias seen in the sample as a result of the exchange couplings. Without these exchange couplings MDM in this sample would also be destroyed, yielding a physical reason for the observed loss of MDM.

Bibliography

Chesnel, K. 2017, Nanoscale Magnetic Domain Memory (intechopen)

Chesnel, K., Safsten, A., Rytting, M., & Fullerton], E. E. 2016, Nature Communications, 1